

# Titanium Dioxide Nanoparticle Exposure Provokes Greater Lung Inflammation in Females Than Males in the Context of Obesity

Ji-Soo Jeong<sup>1,\*</sup>, Hyun Jegal<sup>2,\*</sup>, Je-Won Ko<sup>1,\*</sup>, Jeong-Won Kim<sup>1,3</sup>, Jin-Hwa Kim<sup>1</sup>, Eun-Hye Chung<sup>1</sup>, So-Young Boo<sup>1</sup>, Su-Ha Lee<sup>1</sup>, Ga-Won Lee<sup>2,4</sup>, Se-Myo Park<sup>2</sup>, Mi-Sun Choi<sup>2</sup>, Hyoung-Yun Han<sup>2,4</sup>, Tae-Won Kim<sup>1</sup>

<sup>1</sup>College of Veterinary Medicine (BK21 FOUR Program), Chungnam National University, Daejeon, 34131, Republic of Korea; <sup>2</sup>Department of Predictive Toxicology, Korea Institute of Toxicology, Daejeon, 34114, Republic of Korea; <sup>3</sup>Division of Radiation Biomedical Research, Korea Institute of Radiological and Medical Science, Seoul, 01812, Republic of Korea; <sup>4</sup>Department of Human and Environmental Toxicology, University of Science & Technology, Daejeon, 34113, Republic of Korea

\*These authors contributed equally to this work

Correspondence: Hyoung-Yun Han; Tae-Won Kim, Email hanhy@kitox.re.kr; taewonkim@cnu.ac.kr

**Background:** Obesity is a chronic metabolic disease responsible for causing various health problems. Obese individuals experience disrupted homeostasis, thus making them more vulnerable to environmental pollutants. This study investigated the effect of pre-existing obesity on respiratory toxicity and explored whether sex differences exist in the response to titanium dioxide nanoparticles (TiO<sub>2</sub>-NPs), a component of air pollutants.

**Methods:** Male and female mice were fed a normal diet (ND) or a high-fat diet (HFD) for 26 weeks and then intratracheally instilled with TiO<sub>2</sub>-NPs at concentrations of 0, 0.1, 0.2, and 0.4 mg/50 µL on days 1, 4, 6, 9, 11, and 13. Mice were sacrificed 24 h after the final administration.

**Results:** In HFD-fed obese mice, TiO<sub>2</sub>-NPs exposure led to respiratory inflammation through the toll-like receptor 4-mediated mitogen-activated protein kinase signaling pathway and a subsequent inflammatory response induced by oxidative stress. These effects were more pronounced in females than in males, and this was attributed to the higher sensitivity of females to HFD consumption and early depletion of antioxidant defenses.

**Conclusion:** Our findings suggest an increased risk of respiratory toxicity in individuals with pre-existing obesity and highlight that these effects are sex-specific.

**Keywords:** nanoparticles, high-fat diet, respiratory toxicity, oxidative stress, inflammatory response

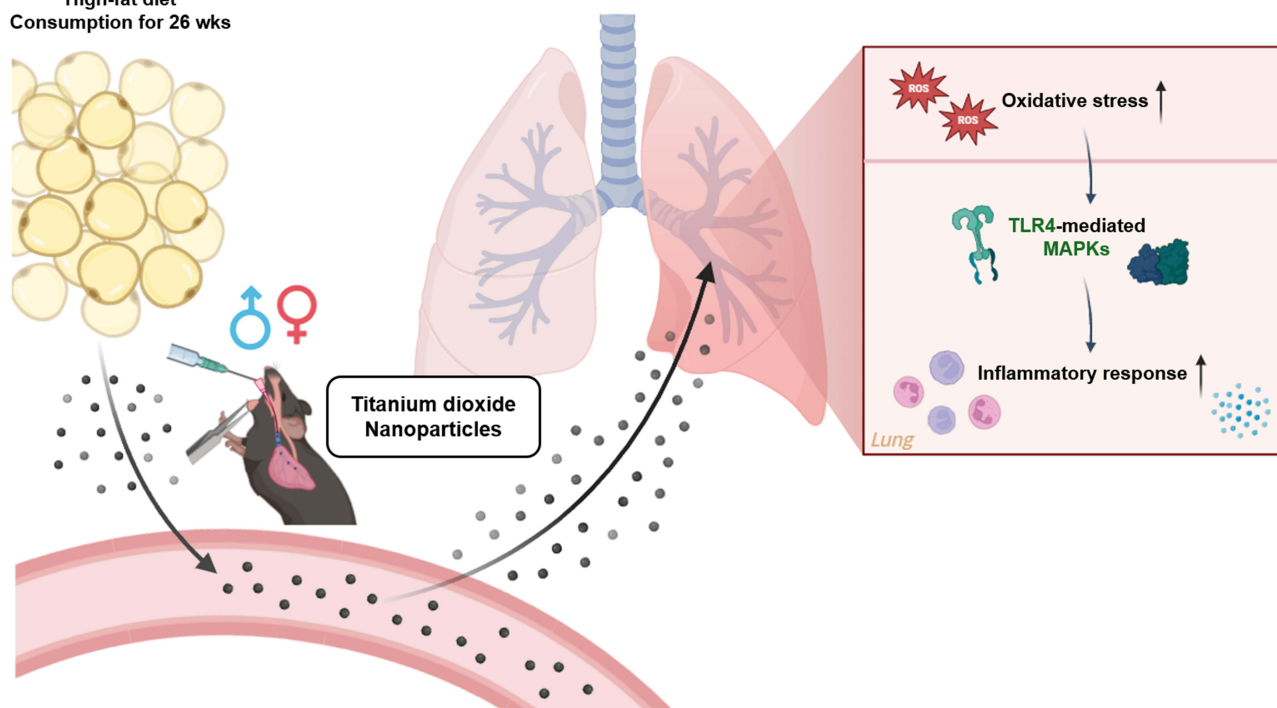
## Introduction

Obesity is defined as the excessive and abnormal accumulation of fat and has emerged as a major public health issue worldwide.<sup>1,2</sup> Obesity leads to a chronic inflammatory state due to the secretion of substances such as cytokines from adipose tissue.<sup>3</sup> Additionally, when adipocytes are exposed to various stressors, including oxidative stress, they trigger an inflammatory response that increases susceptibility to a wide range of diseases such as respiratory disorders.<sup>4</sup> The acceleration of modernization and industrial development has exacerbated air pollution issues and increased the prevalence of respiratory diseases such as chronic obstructive pulmonary disease (COPD) and asthma.<sup>5</sup> Air pollutants enter the human body through inhalation, and the level of harm depends upon both the concentration of the pollutants and the underlying health conditions of the exposed individuals.<sup>6–8</sup> In obesity where systemic molecular and cellular homeostasis is dysfunctional, normal defense mechanisms against air pollutants may be inadequate, thus highlighting the need for further research.<sup>9</sup>

Titanium dioxide (TiO<sub>2</sub>) is widely used at the nanoscale in biomedicine, organic pollutant treatment, materials engineering, and cosmetics.<sup>10</sup> With advances in nanotechnology, greater amounts of TiO<sub>2</sub> nanoparticles (NPs) are being released into the

## Graphical Abstract

High-fat diet  
Consumption for 26 wks



environment.<sup>11,12</sup> In addition to this pollution stemming from industrial increases, Asian sand dust originating from China contains numerous pollutants, particularly submicron-sized particulate matter.<sup>13</sup> Submicron particles of  $\text{TiO}_2$  are highly dispersed within a dust particle matrix.<sup>14</sup> When  $\text{TiO}_2$ -NPs are released into the environment, they remain suspended in the air for extended periods and enter the alveoli through the respiratory system.<sup>15</sup>  $\text{TiO}_2$ -NPs are harmful to human health due to their large surface area and high accumulation in the lungs.<sup>16</sup> Previous studies reported increased levels of various oxidative biomarkers in the respiratory systems of workers involved in the production and handling of  $\text{TiO}_2$ -NPs that led to pathological changes in the lungs.<sup>17,18</sup> Furthermore, the physicochemical properties of  $\text{TiO}_2$ -NPs nanoparticles have been documented to induce dose-dependent airway inflammation and damage.<sup>19–21</sup> However, while research has been conducted examining the inhalation toxicity of  $\text{TiO}_2$ -NPs due to industrial and environmental pollution, reports detailing the risk of respiratory diseases in underlying disorders such as obesity remain lacking.

In this study, we compared and analyzed if exposure to  $\text{TiO}_2$ -NPs, a component of air pollutants,<sup>22</sup> leads to differences in respiratory diseases in the lungs of high-fat diet (HFD)-induced obese and normal diet (ND)-fed mice. We also investigated if these effects varied according to sex.

## Materials and Methods

### Characterization of $\text{TiO}_2$ -NPs

Particle characterization was performed prior to nanotoxicological evaluation.  $\text{TiO}_2$ -NP powder was purchased from Sigma-Aldrich (particle size:  $< 25$  nm; St. Louis, MO, USA). The  $\text{TiO}_2$ -NP samples were diluted to a concentration of 1 mg/mL. The morphology and geometry of  $\text{TiO}_2$ -NPs were investigated using scanning electron microscopy (SU8230, Hitachi, Ltd., Tokyo, Japan). The sizes and shapes of the  $\text{TiO}_2$ -NPs were characterized using transmission electron microscopy (F30 S-Twin, FEI Company, Hillsboro, OR, USA) at an accelerating voltage of 300 kV. The zeta potential and hydrodynamic size of the  $\text{TiO}_2$ -NPs were determined using ELS-8000 (Otsuka Electronic, Tokyo, Japan). The specific surface area of  $\text{TiO}_2$ -NPs was measured by nitrogen absorption techniques on the basis of the multi-point

Brunauer–Emmett–Teller (BET) method (ASAP2020; Micromeritics, Norcross, GA, USA). The purity of the TiO<sub>2</sub>-NPs used in the experiment was determined by energy-dispersive X-ray spectroscopy (EDX-700, Shimadzu, Kyoto, Japan). Endotoxin levels in the TiO<sub>2</sub>-NP suspension were determined using a Pierce LAL Chromogenic Endotoxin Quantitation Kit (Thermo Fisher Scientific, Waltham, MA, USA).

## Animals and Treatment

Five-week-old male and female C57BL/6 mice were obtained from Samtako Inc. (Osan, Korea). The mice were maintained in a clean, well-ventilated animal room with automatically controlled conditions that included a temperature of  $23 \pm 3$  °C, a relative humidity of 30–70%, an approximately 12 h light cycle, and ventilation at 10–20 times/h. After a one-week acclimation period, the experiment was initiated. This study was approved by the Institutional Animal Care and Use Committee of Chungnam National University (202203A-CNU-016), and animal experiments were conducted in accordance with the National Institutes of Health Guide for the Care and Use of Laboratory Animals.

The mice were randomly allocated into six groups, with five mice per group for statistical significance. The experimental groups were conducted separately for both male and female mice. The experimental groups, based on the TiO<sub>2</sub>-NPs administration concentrations determined by referencing previous studies,<sup>23,24</sup> were as follows: 1) ND (Samtako Inc). + TiO<sub>2</sub> 0 mg/mouse; 2) ND + TiO<sub>2</sub> 0.4 mg/mouse; 3) HFD (60 kcal% fat; Samtako Inc). + TiO<sub>2</sub> 0 mg/mouse; 4) HFD + TiO<sub>2</sub> 0.1 mg/mouse; 5) HFD + TiO<sub>2</sub> 0.2 mg/mouse; 6) HFD + TiO<sub>2</sub> 0.4 mg/mouse. In the HFD-induced obesity mouse model, mice were fed a HFD for 26 weeks, after which TiO<sub>2</sub>-NPs were administered. TiO<sub>2</sub>-NPs were suspended in sterile phosphate-buffered saline (PBS) and sonicated for 10 min at 50/60 hz using a Branson 8210 ultrasonicator (Branson Ultrasonics Co., Danbury, CT, USA). Mice were administered sterile PBS or TiO<sub>2</sub>-NPs via intratracheal instillation under gas anesthesia with 3% isoflurane in 100% oxygen, at a volume of 50 µL per mouse, according to the assigned dose for each experimental group, on days 1, 4, 6, 9, 11, and 13. All mice were sacrificed at 24 h after the final administration.

## Bronchoalveolar Lavage Fluid (BALF) Analysis

BALF was obtained to evaluate toxicant-induced alterations in cellular influx.<sup>25</sup> Referring to a previous study,<sup>26</sup> the lungs of the mice were washed with 700 µL of ice-cold sterile PBS through a tracheal cannula, and this process was repeated twice to collect BALF samples (total volume 1.4 mL). The collected BALF was centrifuged, and the supernatant was used to analyze the pro-inflammatory cytokines interleukin (IL)-1 $\beta$ , IL-6, and tumor necrosis factor (TNF)- $\alpha$  using enzyme-linked immunosorbent assay (ELISA) kits (RayBiotech, Peachtree Corners, GA, USA) according to the manufacturer's protocol.

The remaining cell pellet was suspended in 500 µL of PBS. A 200 µL volume of the solution was used to analyze intracellular reactive oxygen species (ROS) levels. The cells were stained with the cell-permeant reagent 2',7'-dichlorofluorescein diacetate (DCFDA; Abcam, Waltham, MA, USA) according to the manufacturer's protocol, attached to a slide using a cytospin (Hanil Scientific Inc., Seoul, Korea), and examined using confocal microscopy (Leica, Wetzlar, Germany) with a 488 nm laser.

For the analysis of inflammatory cells, 200 µL of the solution was attached to a slide using a cytospin and stained with Diff-Quik<sup>®</sup> reagent (Sysmex Co., Kobe, Japan) for cell counting analysis. Another 100 µL of the solution was used for cell population analysis by flow cytometry. The cells were stained with PerCP-CD45, PE-CD11c, APC-SiglecF, and FITC-Ly6G antibodies (BD Biosciences, Franklin Lakes, NJ, USA, 1:100 dilution) in the dark at 4 °C for 30 min. The cells were washed twice with ice-cold PBS and analyzed using a BD Accuri<sup>™</sup> C6 instrument (BD Biosciences).

## Biochemical Analysis

For serum biochemical analysis, blood samples were collected in tubes and centrifuged to obtain serum. Serum chemistry parameters were measured using a Toshiba 200FR NEO chemistry analyzer (Toshiba Co., Tokyo, Japan). The concentration of free fatty acids (FFAs) in the serum was measured using an assay kit (Abcam) as previously described.<sup>27</sup> Leptin and adiponectin concentrations were quantified using ELISA kits (Crystal Chem, Elk Grove Village, IL, USA).

## Histopathological Analysis

Lung and liver specimens fixed in 10% neutral buffered formalin were processed, embedded in paraffin, cut into 4  $\mu\text{m}$  thick sections, and stained with hematoxylin/eosin (H&E; TissuePro Technology, Gainesville, FL, USA). Images of stained tissues were captured from randomly selected areas using a digital photomicroscope (Leica).

## Oxidative Stress Markers Analysis

Various oxidative stress-related markers, including malondialdehyde (MDA), reduced glutathione (GSH), catalase, glutathione S-transferase (GST), glutathione peroxidase (GPx), and glutathione reductase (GR) were evaluated in lung tissues using commercial assay kits (Cayman Chemical, Ann Arbor, Michigan, USA). Lung tissues were homogenized in PBS at a ratio of 1:9 (w/v) using a homogenizer (Hangzhou Allsheng Instruments Co., Hangzhou, China) on ice. The homogenates were then centrifuged at  $20,000 \times g$  for 10 min at 4 °C, and the supernatants were used for the assays. The total amount of oxidative stress-related markers in lung samples was normalized based on the protein concentration measured using a BCA protein assay kit (Thermo Fisher Scientific, Waltham, MA, USA).

## Immunohistochemistry (IHC) and Confocal Immunofluorescence Assay

Immunohistochemical detection of inducible nitric oxide synthase (iNOS) and cyclooxygenase (COX)-2 in the lung tissue was performed using an ABC-HRP kit (VectorLabs, Newark, CA, USA) according to the manufacturer's protocol. The lung sections were incubated with primary rabbit monoclonal antibodies against iNOS (Abcam, 1:500 dilution) and COX-2 (Abcam, 1:500 dilution) at room temperature for 2 h. For color development, 3,3'-diaminobenzidine chromogen and hematoxylin were used. A positive reaction was visualized as brown coloration of the cells.

To detect phosphor (p)-p65 and nuclear factor erythroid 2-related factor 2 (Nrf2) expression, lung sections were hydrated, fixed, and permeabilized. They were then incubated with primary rabbit monoclonal antibodies against p-p65 (Cell Signaling Technology, Danvers, MA, USA, 1:500 dilution) and Nrf2 (Cell Signaling Technology, 1:500 dilution) at room temperature for 2 h. Following this, the samples were incubated with Alexa Fluor 488-conjugated goat anti-rabbit IgG antibody (Abcam) at room temperature for 1 h. Cell nuclei were stained with DAPI. Images were acquired with a confocal laser scanning microscope (Leica) using 450 nm (Blue) and 488 nm (Green) lasers.

## Immunoblotting Analysis

Lung tissue was homogenized in cell lysis buffer containing protease and phosphatase inhibitors. After measuring the protein concentration using the BCA method, samples were prepared with equal protein concentrations and separated using sodium dodecyl sulfate-polyacrylamide gel electrophoresis. Western blotting was performed as previously described to compare protein expression levels.<sup>28</sup> The primary antibodies that were used included Nrf2 (Abcam, 1:2000), heme oxygenase-1 (HO-1; Abcam, 1:1000), iNOS (Abcam, 1:1000), COX-2 (Abcam, 1:1000), TNF- $\alpha$  (Abcam, 1:1000), p-p65 (Cell Signaling Technology, 1:1000), total (t)-p65 (Abcam, 1:1000), toll-like receptor 4 (TLR4; Abcam, 1:1000), p-c-Jun N-terminal kinase (p-JNK; Abcam, 1:1000), t-JNK (Abcam, 1:1000), p-p38 (Abcam, 1:1000), t-p38 (Abcam, 1:1000), and  $\beta$ -actin (Cell Signaling Technology, 1:4000). Relative expression values were measured using the ChemiDoc imaging system (Bio-Rad Laboratories, Hercules, CA, USA).

## QuantSeq 3' mRNA Sequencing Analysis

To investigate the effects of HFD intake on lung tissue, we analyzed lung mRNA expression levels. Male and female mice were each subjected to HFD consumption for 13, 26, 39, and 52 weeks. At each time point, five mice were sacrificed to assess the genetic changes in lung tissue associated with prolonged HFD exposure. Total RNA was isolated from lung tissue using TRIzol reagent (Thermo Fisher Scientific). For library construction, the isolated total RNA was processed using the QuantSeq 3' mRNA-seq Library Prep kit FWD (Lexogen, Vienna, Wien, Austria) according to the manufacturer's instructions. Quality control of raw sequencing data was conducted using FastQC v.12.1.<sup>29</sup> Adapter sequences were trimmed, and low-quality reads were filtered out using bbdut v.39.01.<sup>30</sup> The resulting clean reads were mapped to the reference genome using STAR v.2.7.10b.<sup>31</sup> Read quantification was carried out using HTSeq-count



v.2.0.2.<sup>32</sup> The read counts were normalized using the TMM+CPM method with the Python “conorm” package v.1.2.0.<sup>33</sup> Data mining and graphical visualization were performed using ExDEGA software (Ebiogen Inc., Seoul, Korea).

## Statistical Analysis

All data are presented as mean  $\pm$  standard deviation (SD). To evaluate the significance between groups, one-way analysis of variance (ANOVA) was conducted followed by Dunnett’s or Tukey’s multiple comparison test for normally distributed data and the Kruskal–Wallis test for non-normally distributed data. A *p*-value of  $< 0.05$  or  $0.01$  was considered statistically significant. Statistical analyses were performed using GraphPad Prism 9 software (GraphPad Inc., La Jolla, CA, USA). The detailed statistical analysis methods for each dataset are provided in the figure captions.

## Results

### Physicochemical Characterization of TiO<sub>2</sub>-NPs

The physicochemical properties of TiO<sub>2</sub>-NPs are presented in Figure 1. The morphology of the TiO<sub>2</sub>-NPs was analyzed using transmission electron microscopy and scanning electron microscopy. The results indicated that the TiO<sub>2</sub>-NPs had a spherical shape with an agglomerated morphology (Figure 1A and B). The zeta potential of the TiO<sub>2</sub>-NPs was  $-31.8$  mV (Figure 1C). The purity of the TiO<sub>2</sub>-NPs was measured using energy-dispersive X-ray spectroscopy and found to be 23.89% for Ti and 76.11% for O (Figure 1D). The hydrodynamic sizes of TiO<sub>2</sub>-NPs in PBS were  $239.91 \pm 20.94$  nm (Figure 1E). In

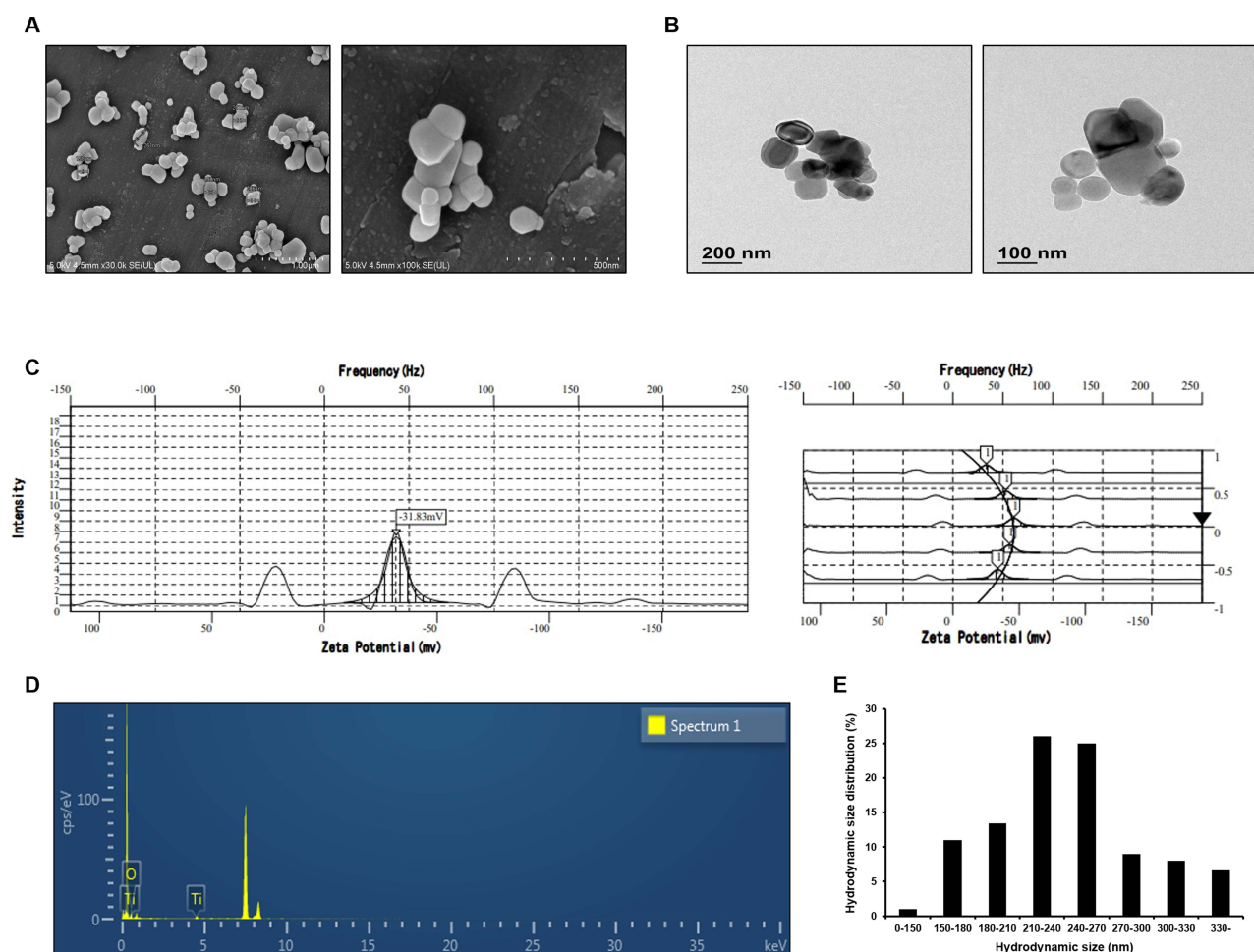


**Figure 1** Morphology and physicochemical properties of titanium dioxide-nanoparticles (TiO<sub>2</sub>-NPs). (A) Morphology of TiO<sub>2</sub>-NPs measured using scanning electron microscopy. Scale bar = 1 μm (left) and 0.5 μm (right). (B) Morphology of TiO<sub>2</sub>-NPs measured using transmission electron microscopy. Scale bar = 200 nm (left) and 100 nm (right). (C) Zeta potential of TiO<sub>2</sub>-NPs measured using ELS-8000. (D) Purity of TiO<sub>2</sub>-NPs measured using energy-dispersive X-ray spectroscopy. (E) Hydrodynamic size of TiO<sub>2</sub>-NPs in phosphate-buffered saline solution measured using ELS-8000.

addition, the surface area of TiO<sub>2</sub>-NPs measured by BET method and single point method was 40.4566 and 39.3805 m<sup>2</sup>/g, respectively (Table S1). TiO<sub>2</sub>-NP suspensions did not contain detectable endotoxin levels (data not shown).

## Effects of HFD Consumption on Biochemical Parameters and Liver Histology in Male and Female Mice

Mice fed a HFD for 16 to 20 weeks typically gain 20–30% more weight than do ND-fed mice, and they exhibit symptoms similar to those of human obesity, including adipocyte hyperplasia and increased fat mass, thus making them a popular model for obesity.<sup>34</sup> In this study, HFD consumption resulted in body weight changes in both male and female mice (Figure 2A). Male and female mice exhibited rapid weight changes beginning at 10 and 15 weeks of HFD exposure, respectively, and no significant differences in body weight changes were observed between sexes.

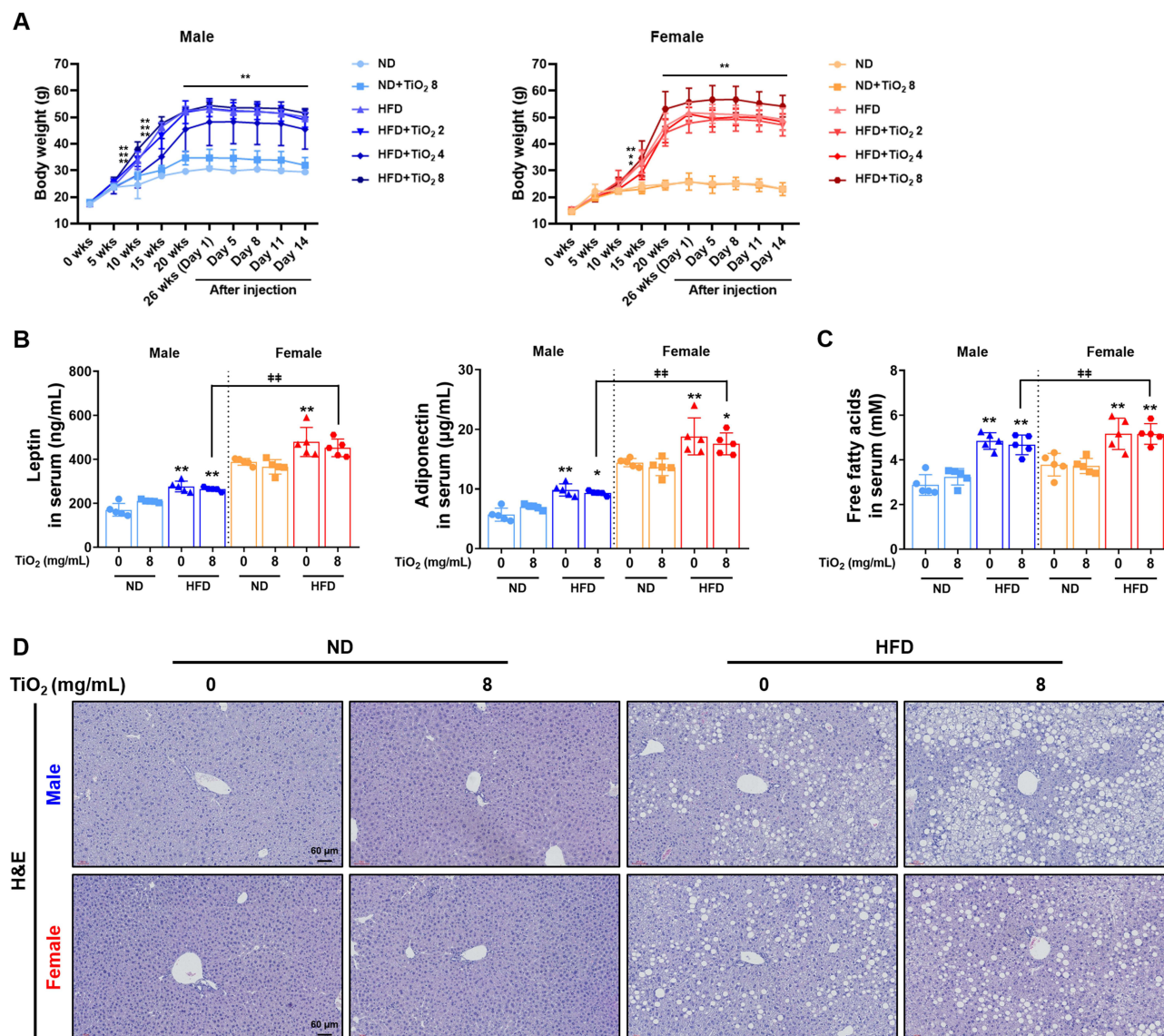


**Figure 2** Effects of a high fat diet (HFD) on male and female mice. **(A)** Changes in body weight. **(B)** Concentrations of leptin and adiponectin in serum measured using enzyme-linked immunosorbent assay. **(C)** Concentrations of free fatty acids (FFAs) in serum measured using a specific assay kit. The concentrations of leptin, adiponectin, and FFAs were increased in the HFD-fed groups and were higher in females than they were in males. **(D)** Histological analysis of liver as confirmed by hematoxylin/eosin (H&E) staining. Scale bar = 60 μm. Lipid droplets were observed in the HFD-fed groups, with no differences between genders or damage caused by titanium dioxide-nanoparticle (TiO<sub>2</sub>-NP) administration. Values: mean ± standard deviation (*n* = 5 per group). Significance: \*,\*\**p* < 0.05 and 0.01 vs Normal diet (ND) control group in each gender, respectively. <sup>#</sup>*p* < 0.01 vs male HFD+TiO<sub>2</sub> 8 mg/mL group. Statistical analysis: Tukey's multiple comparisons test. ND, ND+phosphate-buffered saline (PBS) intratracheal instillation; ND+TiO<sub>2</sub> 8, ND+8 mg/mL/mouse of TiO<sub>2</sub>-NPs intratracheal instillation; HFD, HFD+PBS intratracheal instillation; HFD+TiO<sub>2</sub> 2, 4, and 8, HFD+2, 4, and 8 mg/mL/mouse of TiO<sub>2</sub>-NPs intratracheal instillation, respectively.

Sexual dimorphism in adipokine concentrations was observed in our results, with leptin and adiponectin levels being higher in HFD-fed mice than in ND-fed mice and significantly higher in females than in males (Figure 2B). Serum FFAs concentrations also increased in HFD-fed mice, with higher levels observed in female mice than in male mice (Figure 2C). Serum biochemical analysis exhibited significantly increased levels of inorganic phosphorus, total cholesterol, aspartate aminotransferase, alanine aminotransferase, and phospholipids in HFD-fed males compared to levels in ND-fed males, and significantly increased levels of total cholesterol, aspartate aminotransferase, alanine aminotransferase, phospholipids, and alkaline phosphatase were observed in HFD-fed females compared to levels in ND-fed females (Table S2).

In the livers of mice fed a HFD for 26 weeks, HFD-induced lipid droplets and massive macrosteatosis were observed in both male and female mice compared to these characteristics in ND-fed mice, with no significant differences between the sexes and no effect of TiO<sub>2</sub>-NPs administration (Figure 2D).

## Effects of HFD Consumption Duration on Lung mRNA Expression in Male and Female Mice

To investigate the effects of HFD intake on the lungs according to sex, lung mRNA expression analysis was conducted. Gene expression changes were compared using 13 weeks ND mice of each sex as baseline. HFD consumption exerted a significant impact on the expression of greater number of genes in males. However, as the intake period increased, there were significant changes in the expression of a greater number of genes in females (13 weeks – male: 151, female: 96; 26 weeks – male: 236, female: 214; 39 weeks – male: 175, female: 766; 52 weeks – male: 490, female: 509; total genes: 40,879, fold change > 2.0,  $p < 0.05$ ).

To identify the biological functions associated with these changes in gene expression, we used Database for Annotation, Visualization, and Integrated Discovery (DAVID) analysis.<sup>35</sup> As presented in Figure 3, in males, significant changes were observed in biological processes associated with cellular processes throughout the HFD exposure period, including regulation of transcription by RNA polymerase II (GO:0045944, GO:0000122), regulation of cell population proliferation (GO:0008285), regulation of cell migration (GO:0030335), and regulation of apoptotic process (GO:0043065). In contrast, in females, significant changes were mainly observed in the expression genes related to defense responses to stimuli, including immune response (GO:0006955), immune system process (GO:0002376), inflammatory response (GO:0006954), and chemotaxis (GO:0006935). The list of genes showing significant changes within each GO category are proved in Tables S3–S10.

## Effects of TiO<sub>2</sub>-NPs on Airway Inflammation in Male and Female Mice

To compare the toxicity of TiO<sub>2</sub>-NPs in mice fed ND and HFD, we administered intratracheal instillations of TiO<sub>2</sub>-NPs according to the experimental schedule presented in Figure 4A three times per week for two weeks. Histological analysis of the lung tissue revealed severe infiltration of inflammatory cells around the bronchi in TiO<sub>2</sub>-NPs-treated HFD mice compared to that in mice fed a ND, with more pronounced effects observed in females than in males (Figure 4B). As presented in Figure 4C, the consumption of HFD and administration of TiO<sub>2</sub>-NPs increased ROS levels in the BALF, with this increase being more significant in females than in males. Additionally, when the concentrations of pro-inflammatory cytokines in the BALF were measured by ELISA (Figure 4D), both TiO<sub>2</sub>-NPs-treated ND mice and TiO<sub>2</sub>-NPs-treated HFD mice exhibited a significant increase compared to levels in the ND control group. Notably, the levels of IL-1 $\beta$  and IL-6 increased significantly more in females than they did in males.

Previous studies have reported that TiO<sub>2</sub>-NPs administration induces an influx of leukocytes, with neutrophils being the most abundant among them.<sup>36</sup> Consistent with these findings, our results demonstrated that TiO<sub>2</sub>-NPs administration significantly increased neutrophil counts compared to that of the ND control group, with a greater increase observed in HFD-fed and female mice (Figure 4E). Flow cytometric analysis revealed a similar trend (Figure 4F), showing that TiO<sub>2</sub>-NPs administration increased the proportion of CD45<sup>+</sup>LY6G<sup>+</sup> cells, which are identified as neutrophils. The increase in neutrophils was most pronounced in HFD-fed female mice treated with TiO<sub>2</sub>-NPs, as confirmed by cell count analysis.

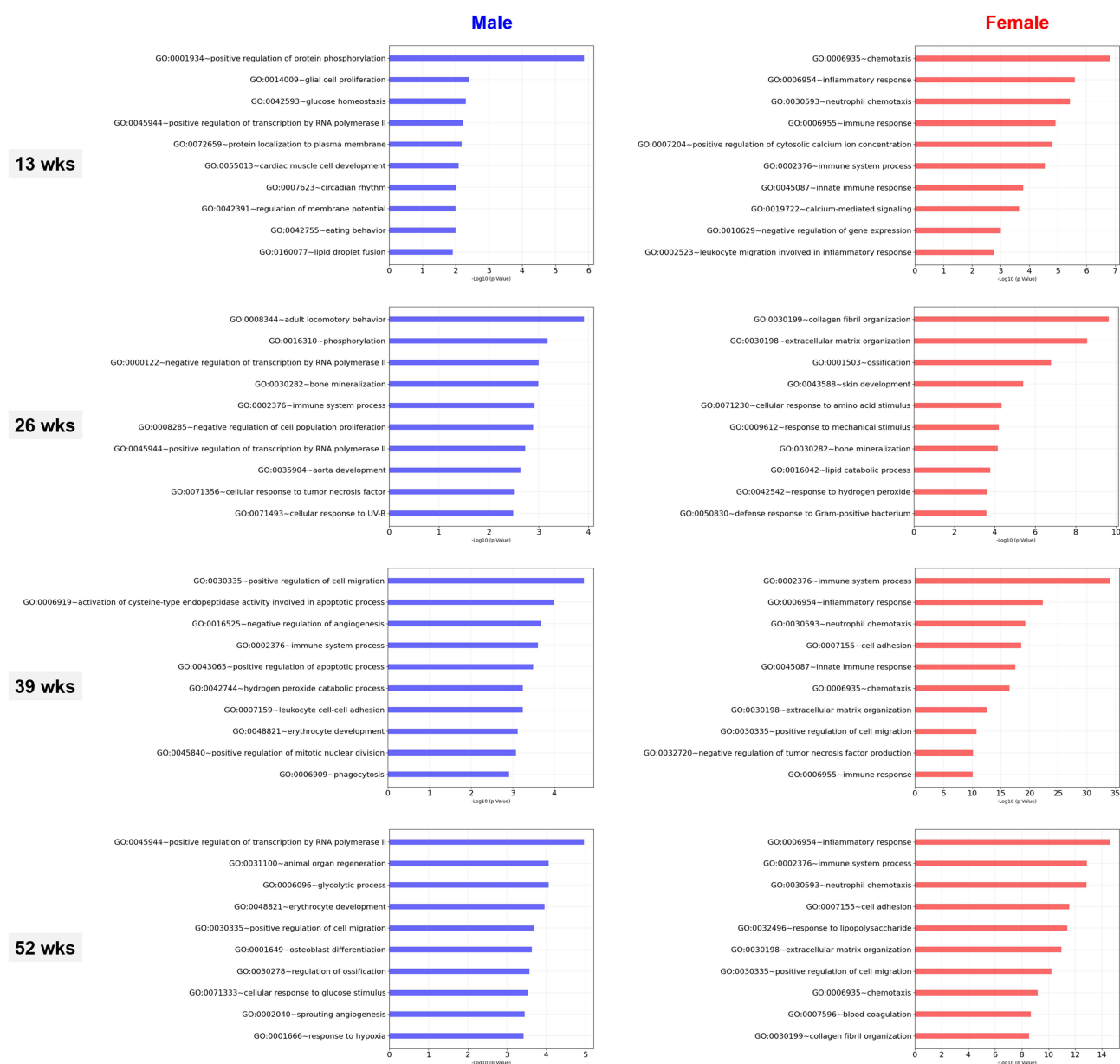


**Figure 3** Effects of a high fat diet on gene expression in the lungs of male and female mice. Database for Annotation, Visualization, and Integrated Discovery (DAVID) functional gene ontology (GO) analysis of biological processes. The top 10 gene categories based on fold change > 2.0 and  $p$ -value < 0.05 compared to levels in mice fed a normal diet for 13 weeks of each gender.

## Effects of TiO<sub>2</sub>-NPs on Inflammatory Response-Related Factors in Male and Female Mice

To investigate the effects of TiO<sub>2</sub>-NPs exposure on the inflammatory response, various inflammation-related factors were examined. Protein expression levels of inflammatory markers such as iNOS, COX-2, TNF- $\alpha$ , and nuclear factor-kappa B (NF- $\kappa$ B) in the lungs were analyzed (Figure 5A). Both male and female groups exposed to TiO<sub>2</sub>-NPs exhibited increased levels of all four markers compared to levels of the ND control group, with the increase being more pronounced in HFD mice than in ND mice and higher in females than in males. iNOS and COX-2 were tracked by IHC staining, and p65 phosphorylation was observed using confocal microscopy. All exhibited the same trend (Figure 5B and C).

In a previous study, TiO<sub>2</sub>-NPs have been demonstrated to generate an inflammatory response in respiratory epithelium through the TLR4-dependent mitogen-activated protein kinases (MAPKs) signaling pathway.<sup>37</sup> To determine if this



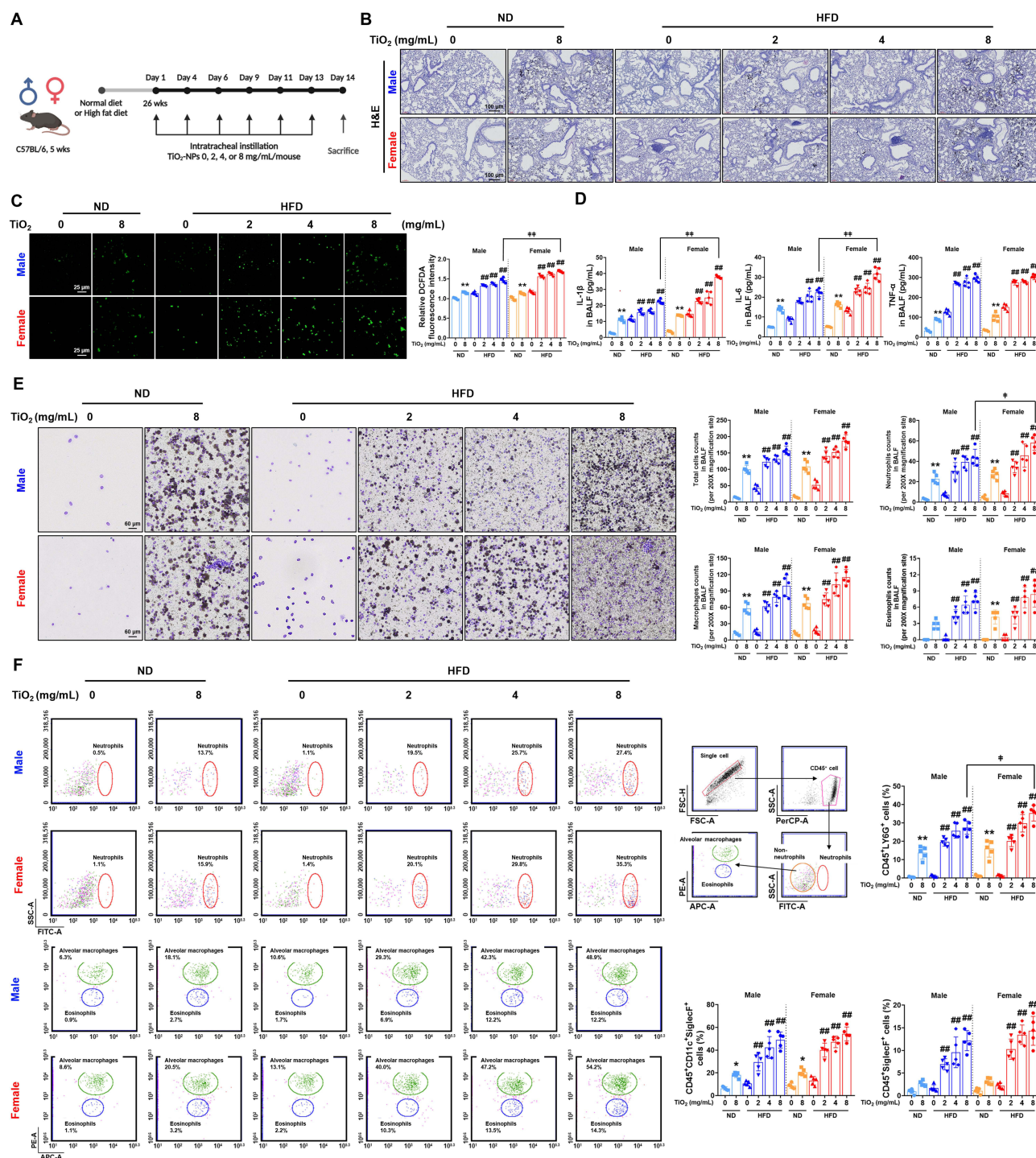


**Figure 4** Effects of titanium dioxide-nanoparticles (TiO<sub>2</sub>-NPs) on the inflammatory phenotype in male and female mice fed either a normal diet (ND) or a high fat diet (HFD). **(A)** Experimental schedule. **(B)** Histological analysis of lung tissue using hematoxylin/eosin (H&E) staining. Scale bar = 100  $\mu$ m. TiO<sub>2</sub>-NPs were dispersed within the lung tissue, and this led to the infiltration of inflammatory cells. This effect was most pronounced in female HFD-fed mice treated with TiO<sub>2</sub>-NPs. **(C)** Representative images of reactive oxygen species (ROS) levels in BALF were measured using the 2',7'-dichlorofluorescein diacetate (DCFDA) reagent and are presented in a quantification graph. Scale bar = 25  $\mu$ m. Both HFD consumption and TiO<sub>2</sub>-NPs exposure increased ROS levels in male and female mice. **(D)** Concentrations of interleukin (IL)-1 $\beta$ , IL-6, and tumor necrosis factor (TNF)- $\alpha$  in bronchoalveolar lavage fluid (BALF) as measured by enzyme-linked immunosorbent assay. The pro-inflammatory cytokines levels were increased by TiO<sub>2</sub>-NPs exposure, with the highest levels observed in the HFD+TiO<sub>2</sub> groups. The extent of this increase was greater in females than it was in males. **(E)** Representative images and quantification graph of Diff-Quick<sup>®</sup> staining of BALF cells. Scale bar = 60  $\mu$ m. **(F)** Representative population dot plot and quantification graph of each inflammatory cell type in BALF as analyzed by flow cytometry, along with the gating strategy used for flow cytometry data analysis. CD45<sup>+</sup> cells, Lymphocyte; CD45<sup>+</sup>LY6G<sup>+</sup> cells, Neutrophils; CD45<sup>+</sup>CD11c<sup>+</sup>SiglecF<sup>+</sup> cells, Alveolar macrophages; CD45<sup>+</sup>SiglecF<sup>+</sup> cells, Eosinophils. TiO<sub>2</sub>-NPs increased the proportion of neutrophils, with the highest levels observed in female HFD mice treated with TiO<sub>2</sub>-NPs. Values: mean  $\pm$  standard deviation ( $n$  = 5 per group). Significance: \*, \*\* $p$  < 0.05 and 0.01 vs ND control group in each gender, respectively. ### $p$  < 0.01 vs ND+TiO<sub>2</sub> 8 mg/mL group in each gender. <sup>†</sup> $p$  < 0.05 and 0.01 vs male HFD+TiO<sub>2</sub> 8 mg/mL group, respectively. Statistical analysis: Tukey's multiple comparisons test. ND, ND+phosphate-buffered saline (PBS) intratracheal instillation; ND+TiO<sub>2</sub> 8, ND+8 mg/mL/mouse of TiO<sub>2</sub>-NPs intratracheal instillation; HFD, HFD+PBS intratracheal instillation; HFD+TiO<sub>2</sub> 2, 4, and 8, HFD+2, 4, and 8 mg/mL/mouse of TiO<sub>2</sub>-NPs intratracheal instillation, respectively.



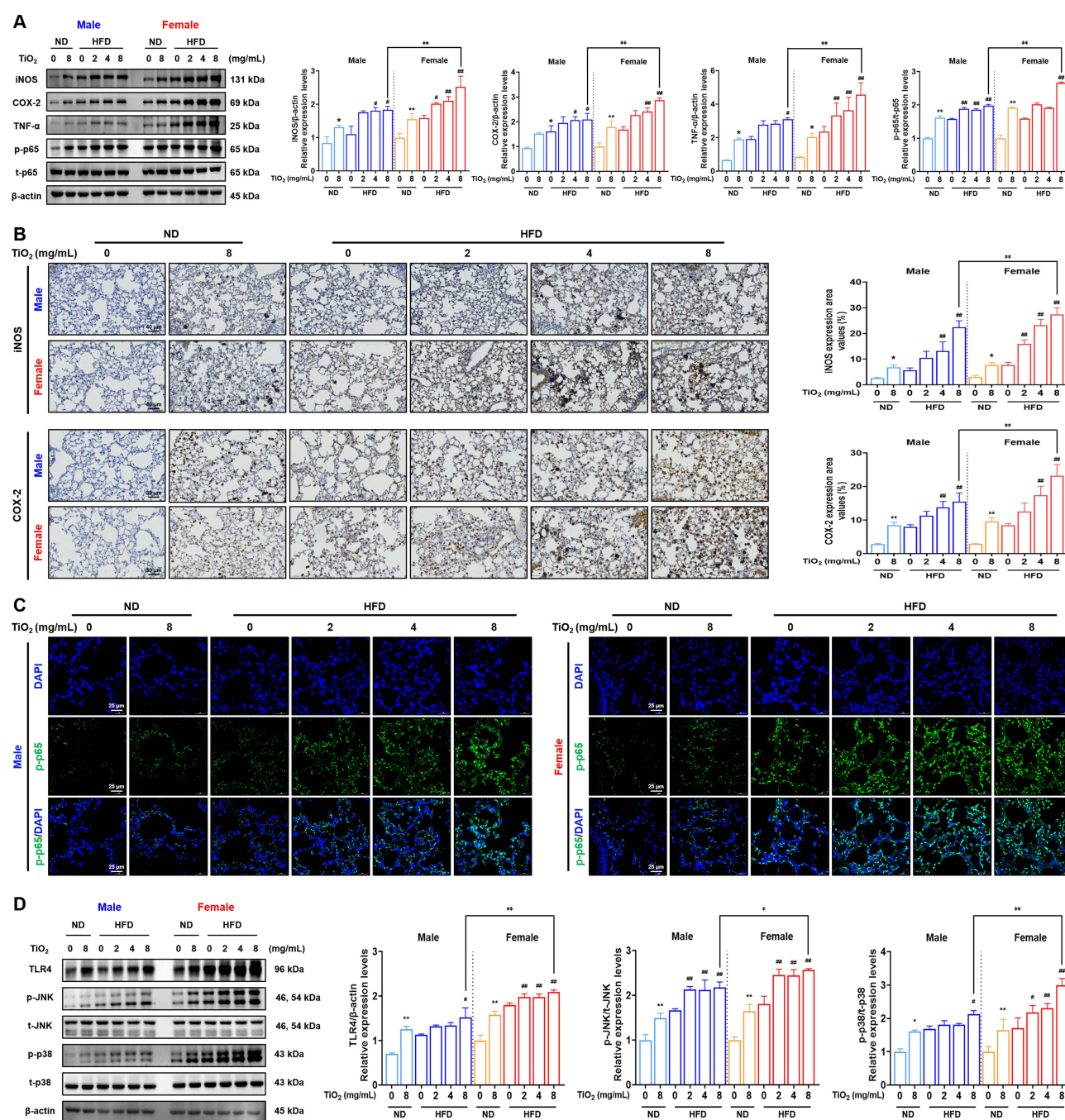


**Figure 5** Effects of titanium dioxide-nanoparticles (TiO<sub>2</sub>-NPs) on the inflammatory response in male and female mice fed either a normal diet (ND) or a high fat diet (HFD). **(A)** Western blot analysis of the indicated proteins in the lung tissue and graphs representing the densitometric values of protein expression. **(B)** Immunohistochemical staining for inducible nitric oxide synthase (iNOS) and cyclooxygenase (COX)-2 in lung tissue and quantification graph. Scale bar = 40  $\mu$ m and 30  $\mu$ m, respectively. **(C)** Immunofluorescence staining for phosphor (p)-p65 in lung tissue. Lung tissues were stained with p-p65 (Green) and DAPI (Blue). Scale bar = 25  $\mu$ m. TiO<sub>2</sub>-NPs exposure increased the expression of inflammation-related factors, with higher expression observed in HFD mice compared to that in ND mice and in females compared to that in males. **(D)** Western blot analysis of the indicated proteins in the lung tissue and graphs representing the densitometric values of protein expression. TNF- $\alpha$ , tumor necrosis factor- $\alpha$ ; t-, total-; TLR4, toll-like receptor 4; JNK, c-Jun N-terminal kinase. Values: mean  $\pm$  standard deviation ( $n = 5$  per group). Significance: \*,\*\* $p < 0.05$  and 0.01 vs ND control group in each gender, respectively. #,### $p < 0.05$  and 0.01 vs ND+TiO<sub>2</sub> 8 mg/mL group in each gender, respectively. <sup>†</sup>,<sup>††</sup> $p < 0.05$  and 0.01 vs male HFD+TiO<sub>2</sub> 8 mg/mL group, respectively. Statistical analysis: Tukey's multiple comparisons test. ND, ND+phosphate-buffered saline (PBS) intratracheal instillation; ND+TiO<sub>2</sub> 8, ND+8 mg/mL/mouse of TiO<sub>2</sub>-NPs intratracheal instillation; HFD, HFD+PBS intratracheal instillation; HFD+TiO<sub>2</sub> 2, 4, and 8, HFD+2, 4, and 8 mg/mL/mouse of TiO<sub>2</sub>-NPs intratracheal instillation, respectively.

pathway was involved in the inflammation induced by TiO<sub>2</sub>-NPs exposure in our experiments, we assessed protein activation via Western blotting (Figure 5D). The expression of TLR4 and phosphorylation of JNK and p38 were increased in mice exposed to TiO<sub>2</sub>-NPs compared to those in ND control mice. This increase was more significant in HFD mice than it was in ND mice, and expression levels were higher in females than they were in males.

## Effects of TiO<sub>2</sub>-NPs on Oxidative Stress-Related Factors in Male and Female Mice

The intake of a HFD and administration of TiO<sub>2</sub>-NPs generates ROS, ultimately leading to oxidative stress in the body.<sup>38</sup> As presented in Figure 6A, we assessed the concentration and activity of factors related to both enzymatic and non-enzymatic oxidative stress markers in lung tissue. MDA levels that are indicative of lipid peroxidation were increased in males in the TiO<sub>2</sub>-NPs-treated HFD groups compared to those in the TiO<sub>2</sub>-NPs-treated ND group. In females, similar to males, an increase in MDA levels was observed in the HFD groups treated with TiO<sub>2</sub>-NPs compared to levels in the ND group with TiO<sub>2</sub>-NPs, with the extent of the increase being higher in females than in males. The concentration of reduced GSH was decreased with TiO<sub>2</sub>-NPs administration and HFD consumption in both male and female mice compared to that in the ND control group, with the lowest levels in HFD-fed mice treated with TiO<sub>2</sub>-NPs. The degree of reduction was greater in females than it was males. The activities of antioxidant enzymes, including catalase, GST, GPx, and GR, in males, the levels were highest in the HFD groups treated with TiO<sub>2</sub>-NPs compared to that in the ND group treated with TiO<sub>2</sub>-NPs. However, in females, the highest levels were observed in the ND group treated with TiO<sub>2</sub>-NPs.

Western blot analysis of the protein expression of other antioxidant enzymes (Nrf2 and HO-1) in the lung tissue revealed that in males, TiO<sub>2</sub>-NPs-treated HFD mice possessed the highest expression levels compared to those of TiO<sub>2</sub>-NPs-treated ND mice. In female mice, the highest expression was observed in TiO<sub>2</sub>-NPs-treated ND mice (Figure 6B). These patterns were corroborated by confocal microscopy that revealed similar trends in the positive fluorescence expression of Nrf2 (Figure 6C). Activated Nrf2 was localized to the nucleus as confirmed by its co-localization with DAPI.

## Discussion

There is growing concern regarding obesity, as it causes a variety of health problems.<sup>39</sup> Additionally, respiratory diseases are on the rise due to industrialization and air pollution.<sup>40</sup> Recent studies have increasingly focused on the effect of underlying diseases on the prevalence of organ disorders. As obese individuals with altered metabolism and homeostasis due to chronic inflammatory conditions caused by excessive fat accumulation may be more vulnerable to external air pollutants, further studies in this area are needed. In the present study, we investigated the impact of obesity as a pre-existing condition on respiratory toxicity and the potential sex differences in these effects using TiO<sub>2</sub>-NPs, a component of air pollutants. Our results demonstrated that, in HFD-fed mice compared to ND-fed mice, TiO<sub>2</sub>-NPs exposure led to increased levels of inflammatory cytokines and ROS in the lungs along with greater upregulation of TLR4-mediated MAPKs expression. These inflammatory responses and the increased expression of inflammation-related proteins are more pronounced in females than they are in males. Regarding antioxidant enzyme activity, males exhibited a compensatory increase due to TiO<sub>2</sub> exposure, whereas females exhibited a decrease in activity due to the early induction of antioxidant responses.

This study focused on evaluating whether there are differences in the effects of inhalation exposure to TiO<sub>2</sub>-NPs on the lungs of HFD-fed mice compared to ND-fed mice and whether there are gender-based differences. Administration of TiO<sub>2</sub>-NPs resulted in their dispersion into the lungs, ultimately leading to the increase in inflammatory cytokines such as IL-1 $\beta$ , IL-6, TNF- $\alpha$ , and neutrophil counts in the BALF. This was accompanied by inflammatory responses and increased ROS levels in the lung tissues. The inflammatory response induced by TiO<sub>2</sub>-NPs was more severe in mice fed a HFD than it was in those fed a ND and was more pronounced in females than it was in males. Lung gene expression analysis demonstrated that exposure to TiO<sub>2</sub>-NPs in HFD-fed mice exhibited sexually dimorphic patterns of induced inflammation. In males, the expression of genes related to cellular processes was prominent by HFD consumption, while in females, the expression of genes related to defense response, such as inflammation and immune responses, was pronounced. HFD can damage epithelial cells<sup>41</sup> that undergo dynamic changes in response to tissue damage.<sup>42</sup> Additionally, an immune response is triggered to protect the tissue from further damage. If this process is not properly controlled, it can lead to an inflammatory response.<sup>43</sup> Considering our results and those of previous studies, there is increased sensitivity to respiratory damage from TiO<sub>2</sub>-NPs in obese states, and this is attributed to epithelial cell damage

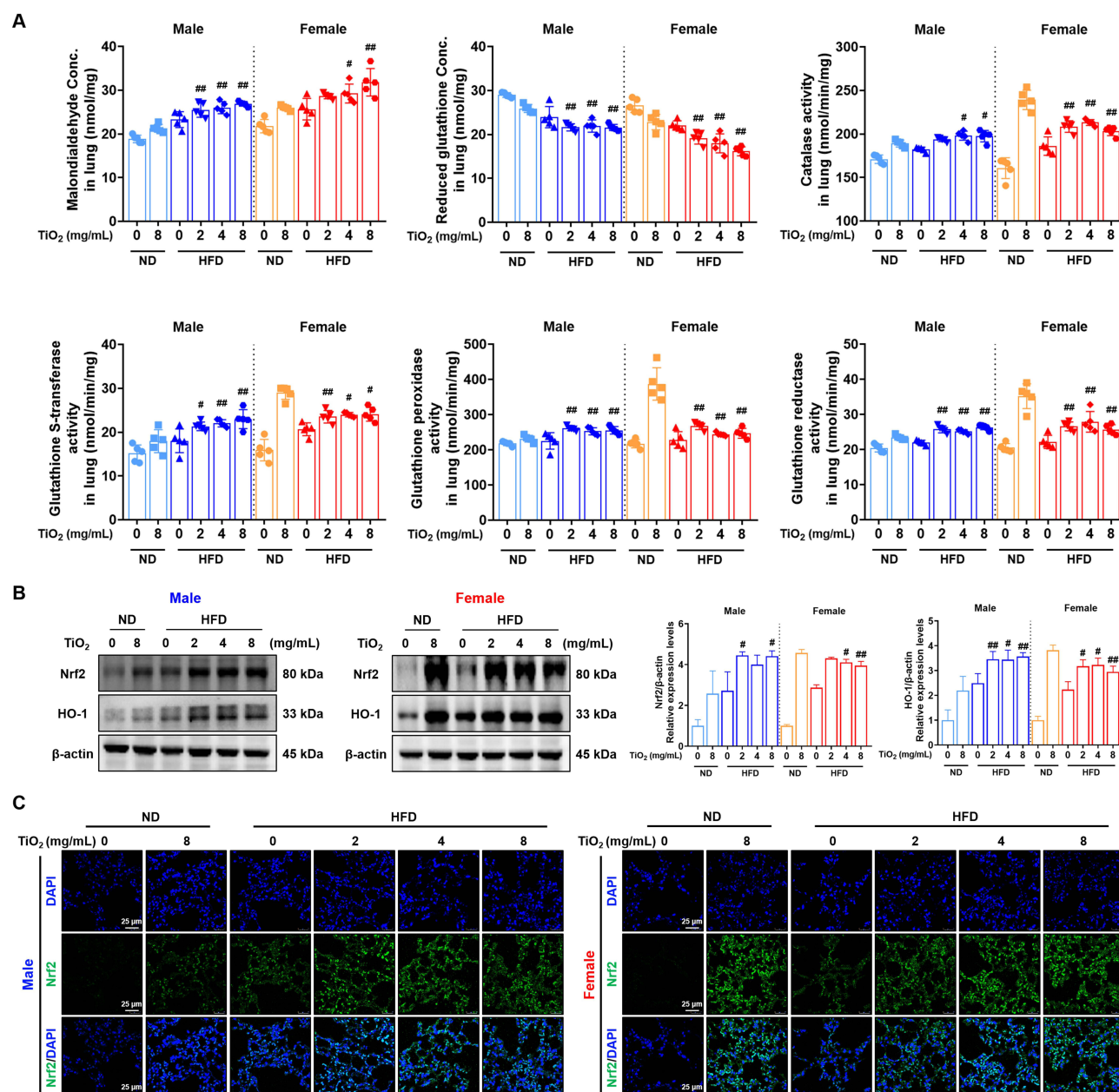


**Figure 6** Effects of titanium dioxide-nanoparticles (TiO<sub>2</sub>-NPs) on oxidative stress in male and female mice fed either a normal diet (ND) or a high fat diet (HFD). **(A)** Concentrations of malondialdehyde (MDA) and reduced glutathione (GSH) and activities of catalase, glutathione S-transferase (GST), glutathione peroxidase (GPx), and glutathione reductase (GR) in lung tissue as measured by assay kit. Values: mean  $\pm$  standard deviation ( $n = 5$  per group). Significance:  $####p < 0.05$  and  $0.01$  vs ND+TiO<sub>2</sub> 8 mg/mL group in each gender, respectively. Statistical analysis: MDA, reduced GSH, catalase, GPx, and GR, by Dunnett's multiple comparisons test for both males and females; GST, by Dunnett's multiple comparisons test for males and Kruskal–Wallis test for females. **(B)** Western blot analysis of the indicated proteins in the lung tissue and graphs representing the densitometric values of protein expression. Significance:  $####p < 0.05$  and  $0.01$  vs ND+TiO<sub>2</sub> 8 mg/mL group in each gender, respectively. Statistical analysis: Dunnett's multiple comparisons test for both males and females. **(C)** Immunofluorescence staining for nuclear factor erythroid 2-related factor 2 (Nrf2) in lung tissue. Lung tissues were stained with Nrf2 (Green) and DAPI (Blue). Scale bar = 25  $\mu$ m. The antioxidant response increased with HFD consumption and exposure to TiO<sub>2</sub>-NPs in males but was highest in the ND+TiO<sub>2</sub> group and slightly decreased in the HFD+TiO<sub>2</sub> groups in females. HO-1, heme oxygenase-1. ND, ND+phosphate-buffered saline (PBS) intratracheal instillation; ND+TiO<sub>2</sub> 8, ND+8 mg/mL/mouse of TiO<sub>2</sub>-NPs intratracheal instillation; HFD, HFD+PBS intratracheal instillation; HFD+TiO<sub>2</sub> 2, 4, and 8, HFD+2, 4, and 8 mg/mL/mouse of TiO<sub>2</sub>-NPs intratracheal instillation, respectively.

induced by HFD. Additionally, females are more sensitive to inflammatory responses from HFD consumption, thus making them more vulnerable to respiratory toxicity in obese states.

To investigate the inflammatory response mechanisms induced by TiO<sub>2</sub>-NPs exposure, we examined the protein expression of relevant factors and observed a TiO<sub>2</sub>-NPs dose-dependent increase in inflammatory proteins such as iNOS, COX-2, TNF- $\alpha$ , and NF- $\kappa$ B. In obesity, a systemic inflammatory response is triggered by increased adipose tissue.<sup>44</sup>



When the homeostasis of lipid metabolism is disrupted in obesity, large amounts of FFAs can act as endogenous ligands for TLRs, thereby activating TLR-dependent signaling cascades that can induce inflammatory responses by producing pro-inflammatory cytokines.<sup>45</sup> The inflammatory response that occurs in obesity is sex-specific, and it has been reported that females are more prone to systemic inflammation due to increased adiposity, with an increased number and size of adipocytes.<sup>46,47</sup> In obese individuals in a systemic inflammatory state, exposure to TiO<sub>2</sub>-NPs may induce inflammation. Recent studies have reported that NPs induce immunotoxicity via MAPK/NF- $\kappa$ B in the TLR downstream signaling cascade.<sup>48,49</sup> Additionally, pulmonary exposure to NPs has been demonstrated to induce more pronounced inflammatory and other pulmonary responses in female mice than those in male mice.<sup>50</sup> In this study, we confirmed that the expression levels of TLR4 and the downstream signaling pathway MAPKs increased dose-dependently in the TiO<sub>2</sub>-NPs-treated groups, with a more significant increase in the HFD-fed mice than was observed in the ND-fed mice. Additionally, the increase was higher in females than it was in males. Overall, respiratory inflammation induced by TiO<sub>2</sub>-NPs is mediated through TLR4-dependent MAPKs signaling pathways, and females with obesity are more vulnerable to respiratory inflammation than are males.

As an upstream pathway of the inflammatory response, oxidative stress generates ROS that increase the transcription of inflammatory mediators through intracellular signaling pathways.<sup>51</sup> HFD causes damage at the cellular and molecular levels and triggers oxidative stress processes.<sup>52</sup> Additionally, oxidative stress is a key factor in the exacerbation of lung pathology through airway inflammation, particularly when exposed to respiratory-specific substances.<sup>53,54</sup> To prevent cellular damage caused by ROS, the body possesses endogenous defense mechanisms that include both non-enzymatic and enzymatic antioxidants that protect against the harmful effects of oxidative stress.<sup>55</sup> Our findings demonstrated that in males, HFD intake was associated with increased MDA concentrations, decreased GSH levels, and increased catalase, GST, GPx, and GR activities. Administration of TiO<sub>2</sub>-NPs further induced oxidative stress that in turn activated these defense mechanisms. However, in females who were more affected by HFD consumption, the antioxidant response was induced earlier by the HFD, and activation appeared to be reduced by the time of observation after TiO<sub>2</sub>-NPs exposure. Consequently, unlike males, female HFD-fed mice treated with TiO<sub>2</sub>-NPs exhibited reduced antioxidant enzyme activity compared to that of female ND-fed mice treated with TiO<sub>2</sub>-NPs. These effects were also observed in the Nrf2/HO-1 pathway, a key regulatory pathway in the cellular defense against oxidative stress.<sup>56</sup> Collectively, the inflammatory response appears to be due to the oxidative stress caused by TiO<sub>2</sub>-NPs exposure, and TiO<sub>2</sub>-NPs administration in the obese state seems to lead to more severe inflammatory responses in females due to the early activation and depletion of cellular protective mechanisms induced by HFD consumption.

One limitation of this study is the use of intratracheal instillation instead of inhalation exposure to evaluate the pulmonary toxicity of TiO<sub>2</sub>-NPs. Although inhalation is the most physiologically relevant route for assessing real-world respiratory exposure, as a more practical alternative, intratracheal instillation was selected due to its relative simplicity and widespread use in non-clinical toxicological studies, particularly those involving nanoparticles, airborne pollutants, and fine particulate matter.<sup>57</sup> Previous research suggests that intratracheal instillation can produce lung toxicity outcomes qualitatively similar to those observed with inhalation exposure, including inflammation, fibrosis, and carcinogenesis.<sup>58</sup> However, notable differences exist between the two methods in terms of deposition patterns, dose delivery, and overall exposure kinetics. These differences should be carefully considered when interpreting the findings and extrapolating them to real-world inhalation scenarios.

## Conclusion

In conclusion, patients with obesity as a pre-existing condition are at a greater risk of respiratory toxicity due to the expression of TLR4-mediated MAPKs and the subsequent inflammatory response induced by oxidative stress. Additionally, this toxicity is more pronounced in females than it is in males due to their increased sensitivity to HFD consumption and early depletion of antioxidant responses. Our results provide important insights into the risk of respiratory toxicity under pre-existing conditions of obesity and highlight the sex differences in these effects.

## Abbreviations

BALF, bronchoalveolar lavage fluid; COX-2, cyclooxygenase-2; DCFDA, 2',7'-dichlorofluorescein diacetate; ELISA, enzyme-linked immunosorbent assay; FFA, free fatty acid; GO, gene ontology; GPx, glutathione peroxidase; GR, glutathione reductase; GSH, glutathione; GST, glutathione S-transferase; H&E, hematoxylin/eosin; HFD, high-fat diet; HO-1, heme oxygenase-1; IHC, immunohistochemistry; IL-, interleukin-; iNOS, inducible nitric oxide synthase; JNK, c-Jun N-terminal kinase; MAPK, mitogen-activated protein kinase; MDA, malondialdehyde; ND, normal diet; NF- $\kappa$ B, nuclear factor-kappa B; NP, nanoparticle; Nrf2, nuclear factor erythroid 2-related factor 2; p-, phosphor-; PBS, phosphate-buffered saline; ROS, reactive oxygen species; t-, total-; TiO<sub>2</sub>, titanium dioxide; TLR4, toll-like receptor 4; TNF-, tumor necrosis factor.

## Ethics Approval

This study was approved by the Institutional Animal Care and Use Committee of Chungnam National University (202203A-CNU-016), and animal experiments were conducted in accordance with the National Institutes of Health Guide for the Care and Use of Laboratory Animals.

## Data Sharing Statement

Data will be made available on request.

## Funding

This work was supported by the National Research Foundation of Korea (NRF) grant funded by the Korean government (MSIT) (No.00211435), the Basic Science Research Program through the National Research Foundation of Korea (NRF) funded by the Ministry of Education (No. 2021R111A3050864), the Nano & Material Technology Development Program (RS-2024-00452934), and the Korea Institute of Toxicology (KIT) Research Program (No. 2710008763).

## Disclosure

The authors declare that they have no known competing financial interests or personal relationships that could have appeared to influence the work reported in this paper.

## References

- Shi X, Zheng Y, Cui H, Zhang Y, Jiang M. Exposure to outdoor and indoor air pollution and risk of overweight and obesity across different life periods: a review. *Ecotoxicol Environ Saf.* **2022**;242:113893. doi:10.1016/j.ecoenv.2022.113893
- Luo C, Wei T, Jiang W, et al. The association between air pollution and obesity: an umbrella review of meta-analyses and systematic reviews. *BMC Public Health.* **2024**;24(1):1856. doi:10.1186/s12889-024-19370-4
- Saltiel AR, Olefsky JM. Inflammatory mechanisms linking obesity and metabolic disease. *J Clin Invest.* **2017**;127(1):1–4. doi:10.1172/JCI92035
- Mafori TT, Rufino R, Costa CH, Lopes AJ. Obesity: systemic and pulmonary complications, biochemical abnormalities, and impairment of lung function. *Multidiscip Respir Med.* **2016**;11:28. doi:10.1186/s40248-016-0066-z
- Jiang XQ, Mei XD, Feng D. Air pollution and chronic airway diseases: what should people know and do? *J Thorac Dis.* **2016**;8(1):E31–40. doi:10.3978/j.issn.2072-1439.2015.11.50
- Daniel AV. *Fundamentals of Air Pollution*. Vol. 43. Cambridge, MA, USA: Academic Press; **2014**:122–215.
- Majumder N, Kodali V, Velayutham M, et al. Aerosol physicochemical determinants of carbon black and ozone inhalation co-exposure induced pulmonary toxicity. *Toxicol Sci.* **2023**;191(1):61–78. doi:10.1093/toxsci/kfac113
- Shetty SS, Deepthi D, Harshitha S, et al. Environmental pollutants and their effects on human health. *Heliyon.* **2023**;9(9):e19496. doi:10.1016/j.heliyon.2023.e19496
- Ghanemi A, Yoshioka M, St-Amand J. Broken energy homeostasis and obesity pathogenesis: the surrounding concepts. *J Clin Med.* **2018**;7(11):453. doi:10.3390/jcm7110453
- Jia X, Wang S, Zhou L, Sun L. The potential liver, brain, and embryo toxicity of titanium dioxide nanoparticles on mice. *Nanoscale Res Lett.* **2017**;12(1):478. doi:10.1186/s11671-017-2242-2
- Nowack B, Bucheli TD. Occurrence, behavior and effects of nanoparticles in the environment. *Environ Pollut.* **2007**;150(1):5–22. doi:10.1016/j.envpol.2007.06.006
- Ray PC, Yu H, Fu PP. Toxicity and environmental risks of nanomaterials: challenges and future needs. *J Environ Sci Health C Environ Carcinog Ecotoxicol Rev.* **2009**;27(1):1–35. doi:10.1080/10590500802708267
- Kang IG, Jung JH, Kim ST. Asian sand dust enhances allergen-induced th2 allergic inflammatory changes and mucin production in BALB/c mouse lungs. *Allergy Asthma Immunol Res.* **2012**;4(4):206–213. doi:10.4168/aa.2012.4.4.206
- Jeong GY. Microanalysis and mineralogy of Asian and Saharan dust. *J Anal Sci Technol.* **2024**;15:10. doi:10.1186/s40543-024-00425-5



15. Rashid MM, Forte Tavčer P, Tomšič B. Influence of titanium dioxide nanoparticles on human health and the environment. *Nanomaterials*. 2021;11(9):2354. doi:10.3390/nano11092354
16. Dar GI, Saeed M, Wu A. *TiO<sub>2</sub> Nanoparticles: Applications in Nanobiotechnology and Nanomedicine*. Hoboken, NJ, USA: Wiley; 2020:67–103.
17. Pelclova D, Zdimal V, Fenclova Z, et al. Markers of oxidative damage of nucleic acids and proteins among workers exposed to TiO<sub>2</sub> (nano) particles. *Occup Environ Med*. 2016;73(2):110–118. doi:10.1136/oemed-2015-103161
18. Pelclova D, Zdimal V, Kacer P, et al. Markers of lipid oxidative damage among office workers exposed intermittently to air pollutants including nanoTiO<sub>2</sub> particles. *Rev Environ Health*. 2017;32(1–2):193–200. doi:10.1515/reveh-2016-0030
19. Chen HW, Su SF, Chien CT, et al. Titanium dioxide nanoparticles induce emphysema-like lung injury in mice. *FASEB J*. 2006;20(13):2393–2395. doi:10.1096/fj.06-6485fje
20. Warheit DB, Webb TR, Reed KL, Frerichs S, Sayes CM. Pulmonary toxicity study in rats with three forms of ultrafine-TiO<sub>2</sub> particles: differential responses related to surface properties. *Toxicology*. 2007;230(1):90–104. doi:10.1016/j.tox.2006.11.002
21. Johnston HJ, Hutchison GR, Christensen FM, Peters S, Hankin S, Stone V. Identification of the mechanisms that drive the toxicity of TiO<sub>2</sub> particulates: the contribution of physicochemical characteristics. *Part Fibre Toxicol*. 2009;6:33. doi:10.1186/1743-8977-6-33
22. Lee SJ, Pak SW, Kim WI, et al. Silibinin suppresses inflammatory responses induced by exposure to Asian sand dust. *Antioxidants*. 2024;13(10):1187. doi:10.3390/antiox13101187
23. Shi H, Magaye R, Castranova V, Zhao J. Titanium dioxide nanoparticles: a review of current toxicological data. *Part Fibre Toxicol*. 2013;10:15. doi:10.1186/1743-8977-10-15
24. Lim JO, Lee SJ, Kim WI, et al. Titanium dioxide nanoparticles exacerbate allergic airway inflammation via TXNIP upregulation in a mouse model of asthma. *Int J Mol Sci*. 2021;22(18):9924. doi:10.3390/ijms22189924
25. Poitout-Belissent F, Grant SN, Tepper JS. Aspiration and inspiration: using bronchoalveolar lavage for toxicity assessment. *Toxicol Pathol*. 2021;49(2):386–396. doi:10.1177/0192623320929318
26. Kim JW, Kim JH, Jeong JS, et al. Green tea extract suppresses airway inflammation via oxidative stress-driven MAPKs/MMP-9 signaling in asthmatic mice and human airway epithelial cells. *Front Immunol*. 2021;15:1362404. doi:10.3389/fimmu.2024.1362404
27. Bocco BMLC, Fernandes GW, Fonseca TL, Bianco AC. Iodine deficiency increases fat contribution to energy expenditure in male mice. *Endocrinology*. 2020;161(12):bqaa192. doi:10.1210/endo/bqaa192
28. Jeong JS, Kim JW, Kim JH, Kim CY, Ko JW, Kim TW. Protective effects of Chestnut (*Castanea crenata*) inner shell extract in macrophage-driven emphysematous lesion induced by cigarette smoke condensate. *Nutrients*. 2023;15(2):253. doi:10.3390/nu15020253
29. Andrews S. FastQC: a quality control tool for high throughput sequence data; 2010. Available from: <http://www.bioinformatics.babraham.ac.uk/projects/fastqc>. Accessed April 18, 2025.
30. Bushnell B. BMAP: a fast, accurate, splice-aware aligner. No. LBNL-7065E. Ernest Orlando Lawrence Berkeley National Laboratory. Berkeley, CA; 2014. Available from: <https://sourceforge.net/projects/bbmap/files>. Accessed April 18, 2025.
31. Dobin A, Davis CA, Schlesinger F, et al. STAR: ultrafast universal RNA-seq aligner. *Bioinformatics*. 2013;29(1):15–21. doi:10.1093/bioinformatics/bts635
32. Putri GH, Anders S, Pyl PT, Pimanda JE, Zanini F. Analysing high-throughput sequencing data in Python with HTSeq 2.0. *Bioinformatics*. 2022;38(10):2943–2945. doi:10.1093/bioinformatics/btac166
33. Meshcheryakov G. Conorm; 2021. Available from: <https://gitlab.com/georgym/conorm>. Accessed April 18, 2025.
34. Casimiro I, Stull ND, Tersey SA, Mirmira RG. Phenotypic sexual dimorphism in response to dietary fat manipulation in C57BL/6J mice. *J Diabetes Complications*. 2021;35(2):107795. doi:10.1016/j.jdiacomp.2020.107795
35. DAVID Bioinformatics. National Institutes of Health; 2024. Available from: <https://davidbioinformatics.nih.gov>. Accessed April 18, 2025.
36. Gonçalves DM, Girard D. Titanium dioxide (TiO<sub>2</sub>) nanoparticles induce neutrophil influx and local production of several pro-inflammatory mediators in vivo. *Int Immunopharmacol*. 2011;11(8):1109–1115. doi:10.1016/j.intimp.2011.03.007
37. Kim GO, Choi YS, Bae CH, Song SY, Kim YD. Effect of titanium dioxide nanoparticles (TiO<sub>2</sub> NPs) on the expression of mucin genes in human airway epithelial cells. *Inhal Toxicol*. 2017;29(1):1–9. doi:10.1080/08958378.2016.1267282
38. Li N, Xia T, Nel AE. The role of oxidative stress in ambient particulate matter-induced lung diseases and its implications in the toxicity of engineered nanoparticles. *Free Radic Biol Med*. 2008;44(9):1689–1699. doi:10.1016/j.freeradbiomed.2008.01.028
39. Lin X, Li H. Obesity: epidemiology, pathophysiology, and therapeutics. *Front Endocrinol*. 2021;12:706978. doi:10.3389/fendo.2021.706978
40. Tran HM, Tsai FJ, Lee YL, et al. The impact of air pollution on respiratory diseases in an era of climate change: a review of the current evidence. *Sci Total Environ*. 2023;898:166340. doi:10.1016/j.scitotenv.2023.166340
41. Hegab AE, Ozaki M, Kagawa S, Fukunaga K. Effect of high fat diet on the severity and repair of lung fibrosis in mice. *Stem Cells Dev*. 2021;30(18):908–921. doi:10.1089/scd.2021.0050
42. Kobayashi Y, Tata A, Konkimalla A, et al. Persistence of a regeneration-associated, transitional alveolar epithelial cell state in pulmonary fibrosis. *Nat Cell Biol*. 2020;22(8):934–946. doi:10.1038/s41556-020-0542-8
43. Yang J, Liang C, Liu L, Wang L, Yu G. High-fat diet related lung fibrosis-epigenetic regulation matters. *Biomolecules*. 2023;13(3):558. doi:10.3390/biom13030558
44. Rogero MM, Calder PC. Obesity, inflammation, toll-like receptor 4 and fatty acids. *Nutrients*. 2018;10(4):432. doi:10.3390/nu10040432
45. Boden G. Obesity and free fatty acids. *Endocrinol Metab Clin North Am*. 2008;37(3):635–646, viii–ix. doi:10.1016/j.ecl.2008.06.007
46. Liqiang S, Fang-Hui L, Minghui Q, Haichun C. Threshold effect and sex characteristics of the relationship between chronic inflammation and BMI. *BMC Endocr Disord*. 2023;23(1):175. doi:10.1186/s12902-023-01396-1
47. Muscogiuri G, Verde L, Vetrani C, Barrea L, Savastano S, Colao A. Obesity: a gender-view. *J Endocrinol Invest*. 2024;47(2):299–306. doi:10.1007/s40618-023-02196-z
48. Iavicoli I, Leso V, Fontana L, Bergamaschi A. Toxicological effects of titanium dioxide nanoparticles: a review of in vitro mammalian studies. *Eur Rev Med Pharmacol Sci*. 2011;15(5):481–508.
49. Pinsino A, Russo R, Bonaventura R, Brunelli A, Marcomini A, Matranga V. Titanium dioxide nanoparticles stimulate sea urchin immune cell phagocytic activity involving TLR/p38 MAPK-mediated signalling pathway. *Sci Rep*. 2015;5:14492. doi:10.1038/srep14492
50. Shvedova AA, Kisin ER, Yanamala N, et al. Gender differences in murine pulmonary responses elicited by cellulose nanocrystals. *Part Fibre Toxicol*. 2016;13(1):28. doi:10.1186/s12989-016-0140-x

51. Mittal M, Siddiqui MR, Tran K, Reddy SP, Malik AB. Reactive oxygen species in inflammation and tissue injury. *Antioxid Redox Signal*. 2014;20(7):1126–1167. doi:10.1089/ars.2012.5149
52. Trindade de Paula M, Poetini Silva MR, Machado Araujo S, et al. High-fat diet induces oxidative stress and MPK2 and HSP83 gene expression in *Drosophila melanogaster*. *Oxid Med Cell Longev*. 2016;2016:4018157. doi:10.1155/2016/4018157
53. Ghio AJ, Carraway MS, Madden MC. Composition of air pollution particles and oxidative stress in cells, tissues, and living systems. *J Toxicol Environ Health B Crit Rev*. 2012;15(1):1–21. doi:10.1080/10937404.2012.632359
54. Valavanidis A, Vlachogianni T, Fiotakis K, Loidas S. Pulmonary oxidative stress, inflammation and cancer: respirable particulate matter, fibrous dusts and ozone as major causes of lung carcinogenesis through reactive oxygen species mechanisms. *Int J Environ Res Public Health*. 2013;10(9):3886–3907. doi:10.3390/ijerph10093886
55. Chaudhary P, Janmeda P, Docea AO, et al. Oxidative stress, free radicals and antioxidants: potential crosstalk in the pathophysiology of human diseases. *Front Chem*. 2023;11:1158198. doi:10.3389/fchem.2023.1158198
56. Delgado-Buenrostro NL, Medina-Reyes EI, Lastres-Becker I, et al. Nrf2 protects the lung against inflammation induced by titanium dioxide nanoparticles: a positive regulator role of Nrf2 on cytokine release. *Environ Toxicol*. 2015;30(7):782–792. doi:10.1002/tox.21957
57. Kim IH, Kim JH, Park SW, et al. Repeated intratracheal instillation effects of commonly used vehicles in toxicity studies with mice. *Sci Rep*. 2024;14(1):30393. doi:10.1038/s41598-024-80438-7
58. Driscoll KE, Costa DL, Hatch G, et al. Intratracheal instillation as an exposure technique for the evaluation of respiratory tract toxicity: uses and limitations. *Toxicol Sci*. 2000;55(1):24–35. doi:10.1093/toxsci/55.1.24

## International Journal of Nanomedicine

### Publish your work in this journal

The International Journal of Nanomedicine is an international, peer-reviewed journal focusing on the application of nanotechnology in diagnostics, therapeutics, and drug delivery systems throughout the biomedical field. This journal is indexed on PubMed Central, MedLine, CAS, SciSearch®, Current Contents®/Clinical Medicine, Journal Citation Reports/Science Edition, EMBase, Scopus and the Elsevier Bibliographic databases. The manuscript management system is completely online and includes a very quick and fair peer-review system, which is all easy to use. Visit <http://www.dovepress.com/testimonials.php> to read real quotes from published authors.

Submit your manuscript here: <https://www.dovepress.com/international-journal-of-nanomedicine-journal>

**Dovepress**  
Taylor & Francis Group